# Age of the Youngest Volcanism at Eagle Lake, Northeastern California—$^{40}Ar/^{39}Ar$ and Paleomagnetic Results

By Michael A. Clynne, Andrew T. Calvert, Duane E. Champion, L.J.P. Muffler, Michael G. Sawlan, and Drew T. Downs

Open-File Report 2017–1027

U.S. Department of the Interior
U.S. Geological Survey

U.S. Department of the Interior
RYAN K. ZINKE, Secretary

U.S. Geological Survey
William H. Werkheiser, Acting Director

U.S. Geological Survey, Reston, Virginia: 2017

For more information on the USGS—the Federal source for science about the Earth, its natural and living resources, natural hazards, and the environment—visit http://www.usgs.gov/ or call 1–888–ASK–USGS (1–888–275–8747).

For an overview of USGS information products, including maps, imagery, and publications, visit http://www.usgs.gov/pubprod/.

Any use of trade, firm, or product names is for descriptive purposes only and does not imply endorsement by the U.S. Government.

Although this information product, for the most part, is in the public domain, it also may contain copyrighted materials as noted in the text. Permission to reproduce copyrighted items must be secured from the copyright owner.

Suggested citation:
Clynne, M.A., Calvert, A.T., Champion, D.E., Muffler, L.J.P., Sawlan, M.G., and Downs, D.T., 2017, Age of the youngest volcanism at Eagle Lake, northeastern California—$^{40}Ar/^{39}Ar$ and paleomagnetic results: U.S. Geological Survey Open-File Report 2017–1027, 24 p., https://doi.org/10.3133/ofr20171027.

ISSN 2331-1258 (online)

# Contents



## Figures



## Tables

# Age of the Youngest Volcanism at Eagle Lake, Northeastern California—$^{40}Ar/^{39}Ar$ and Paleomagnetic Results

By Michael A. Clynne, Andrew T. Calvert, Duane E. Champion, L.J.P. Muffler, Michael G. Sawlan, and Drew T. Downs

## Abstract

The age of the youngest volcanism at Eagle Lake, California, was investigated using stratigraphic, paleomagnetic, and $^{40}Ar/^{39}Ar$ techniques. The three youngest volcanic lava flows at Eagle Lake yielded ages of 130.0±5.1, 127.5±3.2 and 123.6±18.7 ka, and are statistically indistinguishable. Paleomagnetic results demonstrate that two of the lava flows are very closely spaced in time, whereas the third is different by centuries to at most a few millennia. These results indicate that the basalt lava flows at Eagle Lake are not Holocene in age, and were erupted during an episode of volcanism at about 130–125 ka that is unlikely to have spanned more than a few thousand years. Thus, the short-term potential for subsequent volcanism at Eagle Lake is considered low.

## Introduction

Eagle Lake, in northeastern California (fig. 1), is one of 14 sites identified for potential future volcanism in the state (Stovall and others, 2014). Miller (1989) suggested that four young-looking volcanic vents and their lava flows at Eagle Lake (one at Penitentiary Flat, one at Brockman Flat, and two on Ice Cave Ridge) were Holocene in age. Subsequent geologic mapping by Grose and others (2008, 2014) reinterpreted all of these young vents and lava flows to be late Pleistocene in age. Precise ages for these lava flows have not been previously determined, leaving open the possibility that they could be Holocene. Knowledge of the age of these volcanic units is important for planning a monitoring schedule for the Eagle Lake volcanic area and deployment of monitoring resources by the California Volcano Observatory. In this report we describe these vents and lava flows, and document their stratigraphy and age using geologic mapping, paleomagnetic directional data, and $^{40}Ar/^{39}Ar$ radiometric dating.

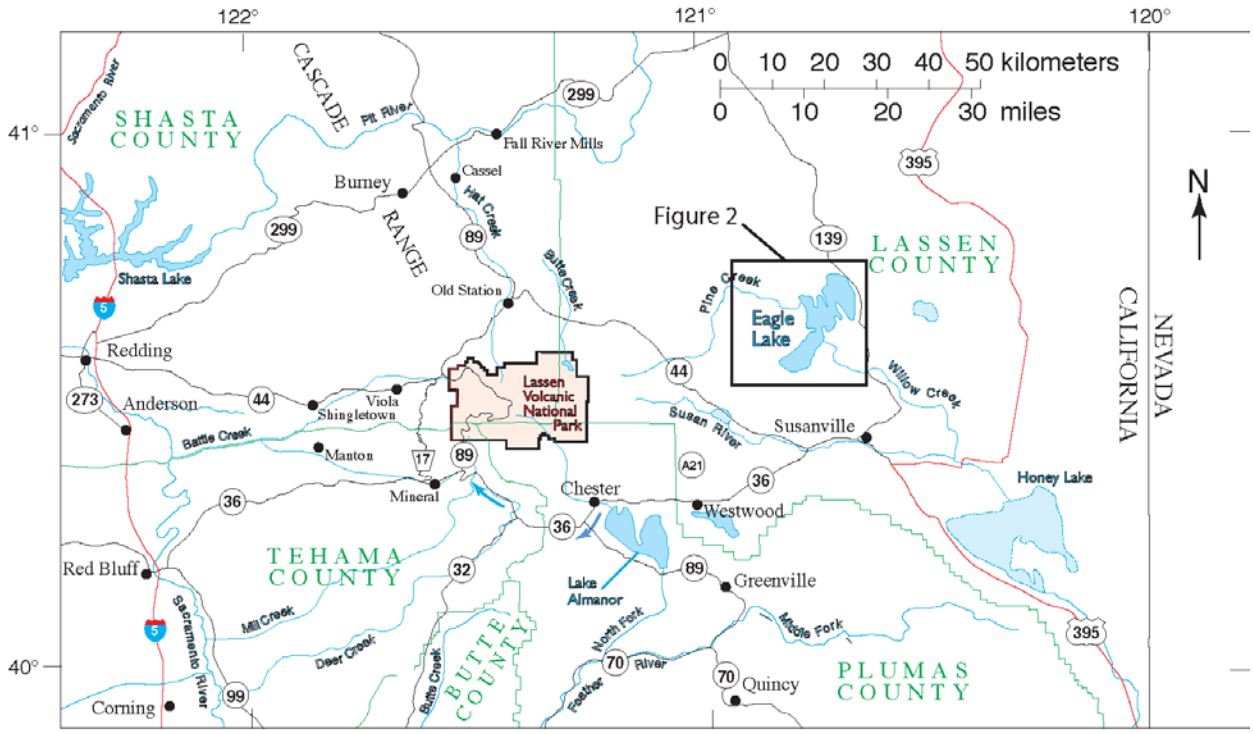


Figure 1. Map showing the location of Eagle Lake in northeastern California (adapted from figure 1 of Muffler and Clynne, 2015). Box around Eagle Lake depicts the area of figure 2.

## General Geology of the Eagle Lake Area

Volcanic rocks in the Eagle Lake area are dominated by Pliocene and older arc-related lavas and pyroclastic deposits (fig. 2) (Grose, 2000; Grose and others, 2008, 2014). These older volcanic rocks are part of the ancestral Cascade arc that has since migrated westward to its present position (Guffanti and others, 1990; Clynne and Muffler, 2010). The most recent volcanism is associated with Basin and Range tectonics and is not part of the active Cascade arc. The young volcanic vents discussed herein are all located along fault traces.

The Eagle Lake area sits along an extension of the eastern Sierra Nevada frontal fault system—a strand of the Walker Lane belt (Faulds and Henry, 2008)—in particular an extension of the Honey Lake Fault, as well as older Basin and Range faulting that cuts most of the Pliocene and older volcanic units (Grose, 2000). The Eagle Lake depression is an irregular, elongate, approximately 8–15 × 22 km transtensional basin created by a combination of normal and right-lateral faulting within the Walker Lane belt (Grose, 2000). Grose (2000) suggested that formation of this lake basin occurred during an episode of faulting in the late Pleistocene, but its precise age remains undetermined. Most of the strongly faulted volcanic units are older than 3 Ma (Grose and others, 2008, 2014). At least part of the lake basin postdates eruption of the basaltic andesite of Black Mountain, dated at 170±70 ka (Grose and McKee, 1986), which forms part of its southeast boundary. Two of the three youngest volcanic units at Eagle Lake partly fill the lake basin.

## Previous Map Depiction of the Young Basalts at Eagle Lake

A number of geologists have conducted studies within the Eagle Lake area, but only the most recent ones are mentioned here. T.L.T. Grose, his students, and colleagues mapped much of the area between 1980 and 2000. That work was compiled into a 1:100,000 scale map and published by the California Geological Survey (Grose and others, 2008, 2014). Grose (2000) also published a summary of this work. Grose and McKee (1986) presented geochronologic data from the area.

Based on our subsequent work, the Grose and others (2008) geologic map depiction of the young basalts at Eagle Lake contains significant inaccuracies. The authors use the unit names basalt of Brockman Flat (Qbb) and older basalt of Brockman Flat (Qbbo), and the vent areas are mapped as a separate unit called volcanic centers (vc and Qbbv). They show three vent locations for the basalt of Brockman Flat. The first, an alignment of vents along the west side of the Eagle Lake basin is correct, with all of the basalt of Brockman Flat now known to be erupted from these vents. The second, an alignment of scoria cones on Ice Cave Ridge and lava flows on the southeast flank of Cave Mountain is incorrect. No part of the basalt of Brockman Flat erupted from vents located on Ice Cave Ridge. The third, a fissure vent (Qbbv) on the east side of Eagle Lake located on the north flank of Black Mountain is said by Grose and others (2014) to be a "local eruptive source" for the basalt of Brockman Flat. No part of the basalt of Brockman Flat erupted from this area either.

Grose and others (2008) correctly identified a vent for the older basalt of Brockman Flat (Qbbo) on Ice Cave Ridge, but incorrectly show the lava flow from that vent overlying the basalt of Brockman Flat (Qbb). They correctly show a lava flow of the older basalt of Brockman Flat (Qbbo) going down the ridge to Pine Creek (the southwest flow described herein). The basalt of Penitentiary Flat is shown as older basalt of Brockman Flat (Qbbo), and is correctly depicted. We present a revised depiction of the stratigraphy and locations of the young basaltic units at Eagle Lake. Our updated mapping is shown in figure 2; we have chosen to emphasize the Eagle Lake basalt lava flows and their ages and do not show faults on the map.

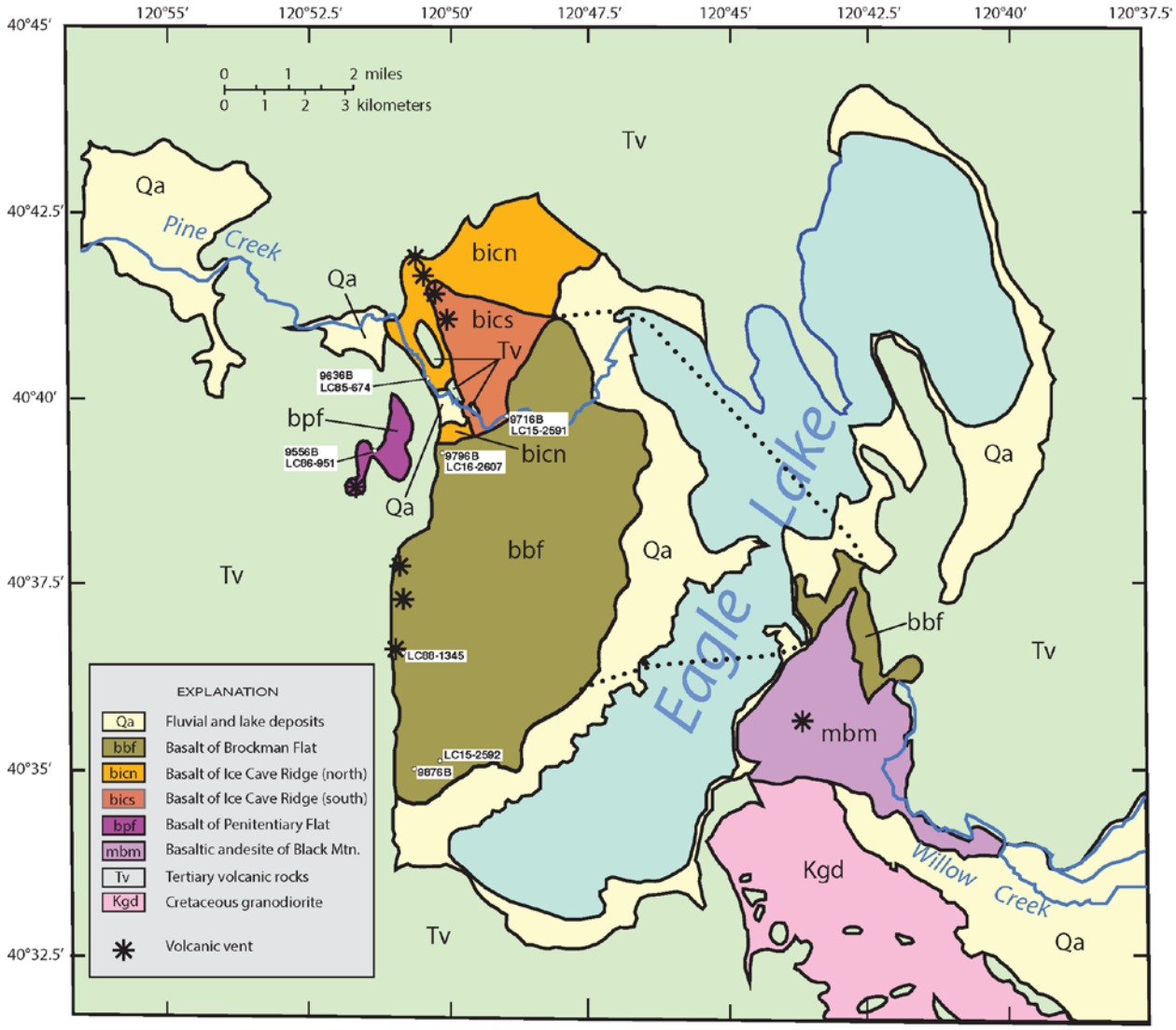


Figure 2. Generalized geologic map showing the location and extent of the young basaltic lava flows at Eagle Lake, northeastern California. Dotted line shows approximate sublacustrine extent of the basalt of Brockman Flat. Modified from Grose and others (2008) based on geologic mapping of M.G. Sawlan and M.A. Clynne. Faults not shown.

## Unit Descriptions

The stratigraphy, petrography, and composition of the three youngest Eagle Lake basalt units are presented in this section. We use the following names to designate these units: (1) basalt of Penitentiary Flat (unit bpf), which is equivalent to the flow of the older basalts of Brockman Flat (unit Qbbo of Grose and others, 2008) at Penitentiary Flat; (2) basalt of Ice Cave Ridge (units bicn and bics), which is equivalent to parts of the older basalts of Brockman Flat (unit Qbbo) and the basalt of Brockman Flat (unit Qbb) of Grose and others (2008); and (3) basalt of Brockman Flat (unit bbf), which is equivalent to part of basalt of Brockman Flat (unit Qbb) as mapped by Grose and others (2008). We include scoria cones and vent areas as part of their associated lava flows and thus do not use the separate units (vc and Qbbv) of Grose and others (2008). The vents and area covered by these basalt units are shown in figure 2. Chemical analyses of the three basalt units are shown in table 1.

Table 1. Representative chemical analyses for basaltic lava flows of Eagle Lake.

[Major elements in weight percent, trace elements in parts per million (ppm). NA, not analyzed; bpf, basalt of Penitentiary Flat; bicn, bicn, basalt of Ice Cave Ridge from the north vents; bics, basalt of Ice Cave Ridge from the south vents; bbf, basalt of Brockman Flat; UTM, universal transverse Mercator;. UTM datum NAD27, zone 10T]

| Sample | LC86-951 | LC85-674 | LC15-2591 | LC88-1345 | LC15-2592 |
|---|---|---|---|---|---|
| Unit | bpf | bicn | bics | bbf vent | bbf flow |
| UTM easting | 0681650 | 0682665 | 0684715 | 0682160 | 0683224 |
| UTM northing | 4502220 | 4504565 | 4503388 | 4497500 | 4494809 |
| $SiO_2$ | 48.94 | 49.78 | 50.44 | 47.77 | 47.98 |
| $Al_2O_3$ | 17.01 | 18.07 | 18.13 | 16.95 | 17.49 |
| $Fe_2O_3$ | 1.52 | 1.51 | 1.96 | 1.63 | 1.54 |
| FeO | 7.76 | 7.68 | 7.07 | 8.32 | 7.87 |
| MgO | 9.58 | 7.13 | 6.80 | 10.67 | 9.63 |
| CaO | 9.93 | 10.24 | 9.14 | 10.27 | 11.43 |
| $Na_2O$ | 3.05 | 3.39 | 3.73 | 2.73 | 2.65 |
| $K_2O$ | 0.59 | 0.55 | 0.86 | 0.36 | 0.21 |
| $TiO_2$ | 1.18 | 1.22 | 1.34 | 0.97 | 0.93 |
| $P_2O_5$ | 0.27 | 0.27 | 0.36 | 0.15 | 0.10 |
| MnO | 0.16 | 0.16 | 0.15 | 0.18 | 0.16 |
| LOI | <0.01 | <0.01 | NA | <0.01 | NA |
| Total | 101.39 | 101.48 | 100.93 | 101.20 | 101.86 |
| FeO*/MgO | 0.95 | 1.27 | 1.30 | 0.92 | 0.93 |
| Mg# | 68.7 | 62.3 | 63.2 | 69.6 | 69.2 |
| Ni | 205 | 100 | 96 | NA | 172 |
| Cr | 434 | 145 | 138 | NA | 213 |
| Rb | 6.5 | 9 | 9 | NA | 9 |
| Sr | 419 | 427 | 496 | NA | 496 |
| Ba | 261 | 267 | 330 | NA | 330 |
| Zr | 151 | 119 | 142 | NA | 61 |

Major element analyses for LC85–LC88 samples performed at USGS Analytical Labs–Denver, Colo., by standard wavelength dispersive x-ray spectrographic methods by analysts David F. Siems and Joseph E. Taggert Jr.; trace elements by energy dispersive x-ray spectroscopy at Menlo Park, Calif., by analyst Peggy Bruggman. For details of sample preparation, analytical procedure, and precision see Clynne and others (2008). Major and trace element analyses for LC15 samples performed at GeoAnalytical Laboratory at Washington State University by standard WDXRF methods. For details of analytical procedure and precision see Johnson and others (1999).

Analyses recalculated to 100 percent anhydrous with $Fe_2O_3$= 0.15x total Fe as $Fe_2O_3$. Total shown is the analytical total prior to recalculation.

### Basalt of Penitentiary Flat (unit bpf)

The basalt of Penitentiary Flat is a ~5-m-thick, 3-km-long lava flow and scoria cone. The unit was previously mapped by Grose and others (2008) as part of the older basalt of Brockman Flat (unit Qbbo). The vent lies along a normal fault cutting the older volcanic rocks, but is not itself, faulted. It has an 'a'ā upper surface with considerable relief. Most of the lava flow is covered with young alluvium derived from the surrounding fault scarps and eolian deposits.

The basalt of Penitentiary Flat is porphyritic olivine basalt containing 8–10 percent olivine and 3–4 percent plagioclase phenocrysts. Olivine phenocrysts are euhedral to subhedral and 0.5–3 millimeters (mm)—mostly 0.5–1 mm—with broad unzoned cores and thin, more iron-rich rims. Some of the larger olivines are embayed, and most contain sparse to abundant inclusions of opaque to dark greenish-brown chromian spinel. Euhedral microphenocrysts of augite are small (as long as ~0.1 mm) and sparse. Euhedral, tabular, calcic plagioclase phenocrysts are mostly <0.5 mm but as long as 1 mm, and they are typically sparsely twinned and weakly zoned. Glomeroporphyritic clots of olivine and plagioclase are sparse and small (generally 1–2 mm). The basalt of Penitentiary Flat has a nearly holocrystalline, pilotaxitic groundmass of plagioclase, pyroxene, olivine and iron-titanium oxide.

### Basalt of Ice Cave Ridge (units bicn, bics)

The basalt of Ice Cave Ridge erupted from a 2-km-long alignment of vents that formed four small scoria cones on Ice Cave Ridge (fig. 2). The vents are aligned along a buried normal fault (Grose and others, 2008). Lava flowed down the slope into the Eagle Lake basin, where it is overlain by lake sediments of two different ages (Grose and others, 2008). Lava flows from the northern two vents (unit bicn) flowed east and southwest. The eastern flow reached at least to the present shore of Eagle Lake and the southwest flow went down the ridge and over the fault scarp into Pine Creek, where it is probably covered by the basalt of Brockman Flat. These flows cover at least 12 square kilometers ($km^2$). The basaltic lava erupted from the southern two vents (unit bics) overlies lava extruded from the northern vents and covers about 6 $km^2$ on the south and east flanks of Ice Cave Ridge. Ice Cave Ridge lava flows have an 'a'ā upper surface. Faults with small offsets cut the lava flows, especially in Pine Creek. The basalt of Ice Cave Ridge is overlain by the basalt of Brockman Flat. Lavas from the north and south vents have subtly different compositions, primarily in the abundances of incompatible major and trace elements (table 1).

The basalt of Ice Cave Ridge is a sparsely porphyritic olivine basalt containing 3–4 percent olivine and 8–10 percent plagioclase phenocrysts. Lavas from the north and south vents are petrographically similar, although glomeroporphyritic clots tend to be larger and perhaps more abundant in the lava flow from the north vents. Olivine phenocrysts are euhedral to subhedral, and 0.25–1.5 mm (mostly 0.5–1 mm) with broad unzoned cores and thin more iron-rich rims. A few of the larger olivines contain sparse to abundant inclusions of opaque to dark-greenish-brown chromian spinel. Euhedral, tabular, calcic plagioclase phenocrysts are 0.25–1.5 mm (mostly 0.5–1 mm); larger phenocrysts as long as 5 mm are rare. Typically, these plagioclase phenocrysts are sparsely twinned and have broad unzoned cores and thin sodic rims, but some plagioclase show weak oscillatory zoning. Plagioclase phenocrysts with finely sieved cores and overgrowth rims are rare. A large proportion of the phenocrysts are in glomeroporphyritic clots of unzoned plagioclase and olivine as long as 5 mm, with a few as long as 1 centimeter (cm). Some clots contain sparse interstitial 0.5–1 mm augite. Some of the plagioclase in these clots has abundant or bent twins suggesting deformation as a result of slight

compaction. This basalt has a nearly holocrystalline, pilotaxitic groundmass of plagioclase, pyroxene, olivine and iron-titanium oxide.

### Basalt of Brockman Flat (unit bbf)

The basalt of Brockman Flat erupted from a north-south oriented 3-km-long fissure vent along a fault that forms the west boundary of the Eagle Lake basin. This eruption built a spatter rampart, and lava was transported in tubes to the north, south, and east, creating an approximately 63-km$^2$ flow field. The lava flowed across the Eagle Lake basin, and small areas crop out on the east side of Eagle Lake and in the headwaters of Willow Creek. The sublacustrine extent of this lava flow is unknown. The lava flow has a weak pāhoehoe surface and is covered with small collapse features and tumuli. This lava flow is overlain by lacustrine sediments along the west shore of Eagle Lake, interpreted by Grose and others (2008) to be Pleistocene and Holocene. Several faults with small offsets cut the lava flow west of Eagle Lake. The composition of the basalt in the spatter rampart is relatively enriched in incompatible elements and phenocrysts compared to the main part of the lava flow (table 1), a characteristic often seen in low-potassium olivine tholeiites (LKOT) in northern California (for example, Turrin and others, 2007).

The basalt of Brockman Flat is a nearly aphyric olivine basalt. It contains very sparse phenocrysts of olivine and plagioclase (olivine > plagioclase). Euhedral olivines (<1 percent) are 0.25–0.75 mm (mostly <0.5 mm) with broad unzoned cores and thin more iron-rich rims. Larger olivines that reach as much as 2 mm are rare and contain sparse inclusions of opaque to dark greenish-brown chromian spinel. Euhedral, calcic plagioclase phenocrysts are very sparse (<<1 percent), 0.5–1.5 mm (mostly about 0.5 mm) and are unzoned with thin sodic rims. Small glomeroporphyritic clots of olivine and plagioclase are rare. The groundmass is a nearly holocrystalline arrangement of plagioclase, pyroxene, olivine and iron-titanium oxide in a coarsely diktytaxitic texture (the average size of plagioclase in the groundmass is about 0.35–0.5 mm). The texture of lava in the spatter rampart contrasts with that of the lava flow. Lava composing the spatter rampart is mostly remobilized spatter and contains as much as ~10 percent phenocrysts of olivine and plagioclase (olivine > plagioclase). Olivines are 0.5–2 mm, but mostly 0.5–1 mm. Many of the larger olivines contain sparse to abundant inclusions of dark-greenish-brown chromian spinel. The calcic plagioclase phenocrysts are tabular, 0.5–3 mm (mostly <1.5 mm), weakly twinned, and unzoned with thin sodic rims. Many of the phenocrysts are present in small glomeroporphyritic clots. The groundmass is a nearly holocrystalline arrangement of plagioclase, pyroxene, olivine and iron-titanium oxide with a fine-grained, weakly diktytaxitic texture (average size of the plagioclase in the groundmass is ~0.1 mm).

## Paleomagnetic Secular Variation

Studies of paleomagnetic secular variation were carried out on the Eagle Lake basalts described above to determine whether they fall into discrete temporal groups, and if so, to provide correlations independent of the field and chemical data sets. Discriminating such temporal groups is difficult to achieve by the $^{40}Ar/^{39}Ar$ method as a result of uncertainties on the order of thousands of years.

Obtaining accurate paleomagnetic directions from uneroded, unglaciated lava flows at Eagle Lake was straightforward, and the sample sets are of high quality. Sample sites were restricted to creek bottoms and road cuts. Paleomagnetic samples were collected, processed and

interpreted using the methods described in McElhinny (1973). Samples were taken in the field using a handheld, gasoline-powered, 2.5 cm coring drill and oriented using a sun compass. Eight, 10-cm-long samples were taken at each site. The 2.5-cm-long specimens were measured using an automated cryogenic magnetometer and subjected to alternating-field (AF) demagnetization to remove secondary components of magnetization. An isothermal component from nearby lightning strikes was a rare, but the most frequent, source of secondary magnetization in these young, volcanic rock units. The characteristic direction of remanent magnetization for each site was calculated using Fisher statistics from line fits of data on equal-area diagrams.

Site mean directions of magnetization for the basalt of Penitentiary Flat, basalt of Ice Cave Ridge, and basalt of Brockman Flat are presented in table 2 and are illustrated in figure 3 for each lava flow as part of an equal-area projection (lower hemisphere) showing mean directions and ovals of 95 percent confidence ($\alpha 95$).

Table 2. Paleomagnetic data for basaltic lava flows of Eagle Lake.

[Lat.(N) and Long.(E), site location in latitude degrees (N), and longitude degrees (E); N/No, the number of cores used compared to the number originally taken at the site; Exp. , Li indicates a line analysis was used on stepwise alternating-field demagnetization data on a vector component diagram; I, remanent inclination in degrees; D, remanent declination in degrees; α95, radius of the 95 percent confidence limit about the mean direction; k, estimate of the Fisher precision parameter; R, length of the resultant vector; Plat.(N) and Plong.(E), location in degrees north and east of the virtual geomagnetic pole (VGP) calculated from the mean direction of the site]

| Unit name | Site | Lat. (N) | Long. (E) | N/No | Exp. | I | D | α95 | κ | R | Plat. (N) | Plong. (E) |
|---|---|---|---|---|---|---|---|---|---|---|---|---|
| Basalt of Penitentiary Flat (bpf) | 9556B | 40.655° | 239.146° | 7/8 | Li | 64.7° | 15.9° | 2.0° | 898 | 6.9933 | 77.1° | 296.4° |
| Basalt of Ice Cave Ridge (bicn) | 9636B | 40.671° | 239.162° | 8/8 | Li | 65.6° | 18.1° | 2.1° | 730 | 7.9904 | 75.3° | 294.3° |
| Basalt of Ice Cave Ridge (bics) | 9716B | 40.663° | 239.185° | 8/8 | Li | 64.4° | 15.4° | 2.1° | 684 | 7.9898 | 77.5° | 297.6° |
| Basalt of Brockman Flat (bbf) | 9796B | 40.655° | 239.162° | 8/8 | Li | 59.1° | 353.1° | 2.1° | 711 | 7.9902 | 84.6° | 142.5° |
| Basalt of Brockman Flat (bbf) | 9876B | 40.584° | 239.157° | 8/8 | Li | 61.1° | 355.2° | 2.3° | 607 | 7.9885 | 86.1° | 174.5° |

Site 9556B is equivalent to LC86-951 in Table 1; Site 9636B is from basalt of Ice Cave Ridge from the north vents and is equivalent to LC85-674; Site 9716B is from basalt of Ice Cave Ridge from the south vents and is equivalent to LC15-2591; Site 9876B is equivalent to the nearby sample LC15-2592. See figure 2 and table 1 for sample locations.

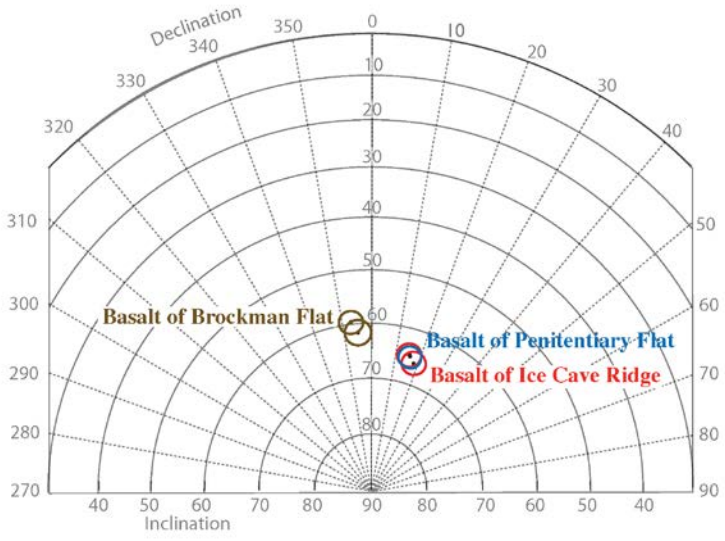


Figure 3. Part of equal-area stereographic projection (lower hemisphere) showing mean directions and ovals of 95 percent confidence on basaltic flows of Eagle Lake. See figure 2 and table 1 for sample locations.

A single determination from the basalt of Penitentiary Flat and two determinations from the basalt of Ice Cave Ridge (one from the north vent flows and one from the south vent flows) have equivalent directions within 95 percent confidence. Two determinations of the magnetic direction from the basalt of Brockman Flat are consistent at the 95 percent confidence and clearly different than the other basalt units.

## $^{40}Ar/^{39}Ar$ Results

Samples were analyzed using the $^{40}Ar/^{39}Ar$ incremental heating technique. Details of the analytical techniques are presented in appendix 1. The incremental heating data and associated 1σ errors are plotted in figure 4, both as age spectrum diagrams and as isotope-correlation (isochron) diagrams. Details of the stepwise heating experiments are given in appendix 2. For the age spectra, apparent ages are calculated assuming that nonradiogenic argon is atmospheric in composition ($^{40}Ar/^{36}Ar = 298.56$, following mass discrimination correction [Lee and others, 2006]), and values are plotted against the cumulative $^{39}Ar$ released during the experiment. In cases with at least three contiguous steps yielding ages within analytical error, we calculated and report plateau ages by weighing individual ages by the inverse of their analytical error.

Application of the $^{40}Ar/^{39}Ar$ techniques to the basalts of Eagle Lake yielded reliable ages that agree with stratigraphic order (table 3). The basalt of Penitentiary Flat yielded a plateau age of 130.0±5.1 ka, the basalt of Ice Cave Ridge from the south vents yielded a plateau age of 127.5±3.2 ka, and the basalt of Brockman Flat yielded a plateau age of 123.6±18.7 ka. Their isochrons, $^{40}Ar/^{36}Ar$ intercepts, and total gas ages are consistent with the plateau ages. Considering their uncertainties, all three of these ages are statistically indistinguishable.

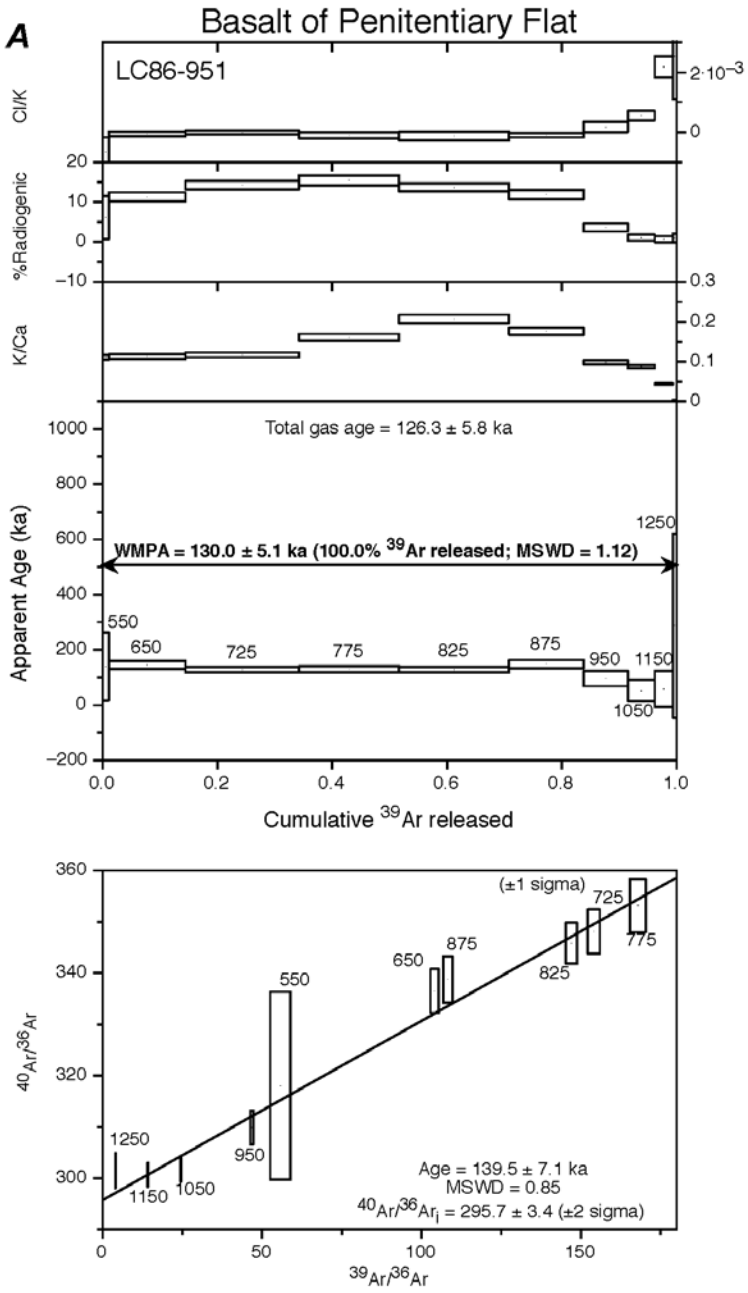


Figure 4. Argon plateau and isochron diagrams for dated Eagle Lake basalt samples. The preferred age in each case is the plateau age. *A*, Sample LC86-951, basalt of Penitentiary Flat. *B*, Sample LC15-2591, basalt of Ice Cave Ridge from the south vents. *C*, Sample LC15-2592, basalt of Brockman Flat. Green line and text indicates isochron that includes only the steps in the plateau age. See table 3 for summary data and appendix 2 for detailed step-heating data. Cl/K, ratio of chlorine to potassium; K/Ca, ratio of calcium to potassium; %, percent; ka, kiloannums or thousands of years; WMPA, weighted mean plateau age; MSWD, mean square of the weighted deviates; $^{40}Ar/^{36}Ari$, $^{40}Ar/^{36}Ar$ intercept at 0 $^{39}Ar/^{36}Ar$; 2s, 2 sigma. See figure 2 and table 1 for sample locations.

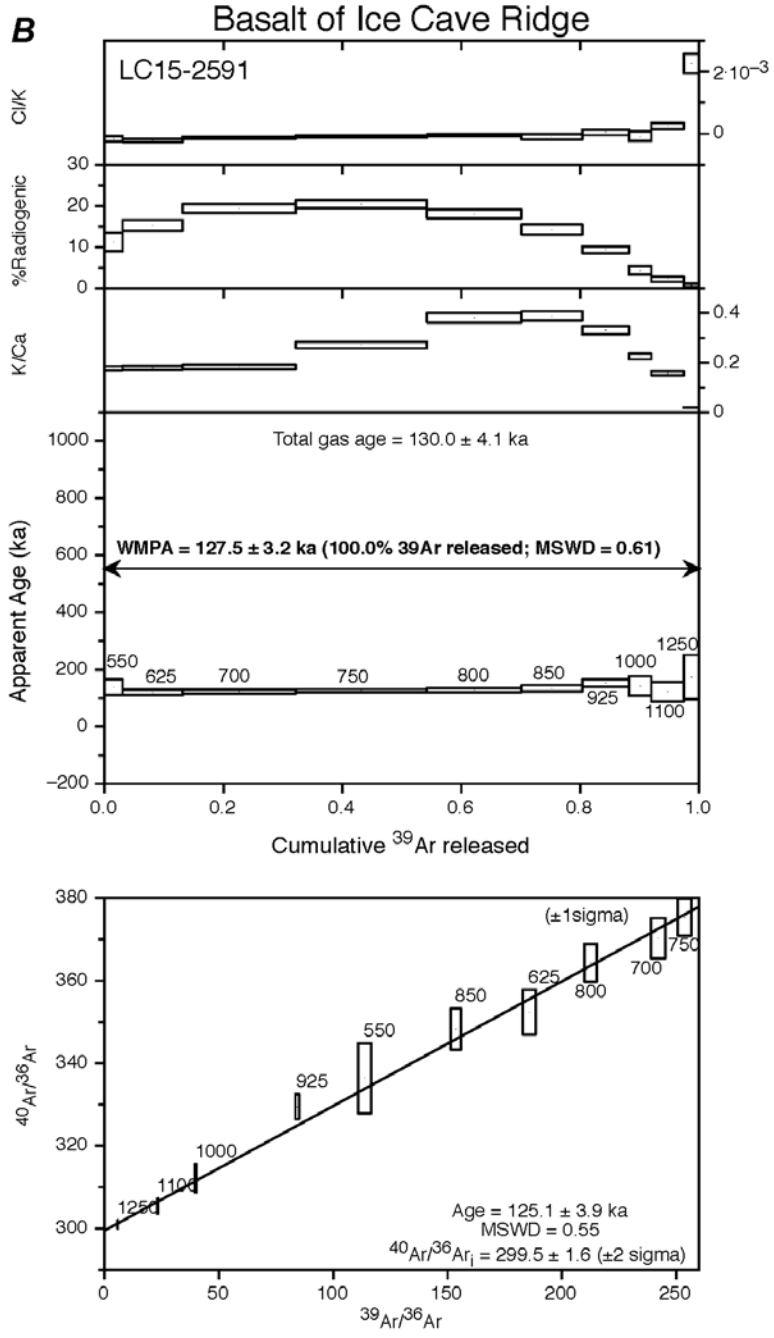


Figure 4.-Continued

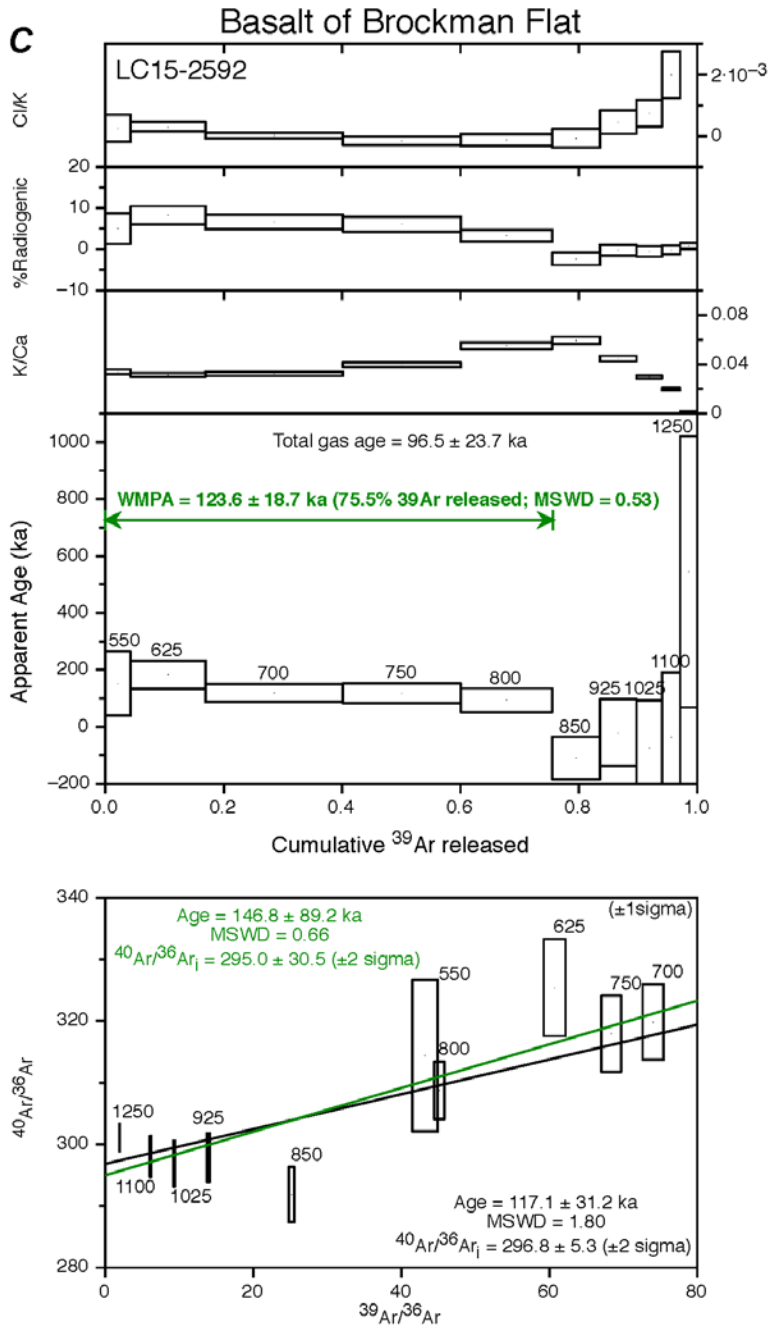


Figure 4.-Continued

Table 3. $^{40}Ar/^{39}Ar$ ages for basaltic lava flows of Eagle Lake, with the preferred ages in bold.

[Exp., experiment; ka, thousands of years; °C, degrees Celsius; MSWD, mean square of the weighted deviates]

| | | | $^{40}Ar/^{39}Ar$ weighted mean plateau age | | | $^{40}Ar/^{39}Ar$ isotope correlation (isochron) age | | | | |
|---|---|---|---|---|---|---|---|---|---|---|
| Sample | Unit | Exp. | Age (ka) | Percent $^{39}Ar$ [steps, °C] | MSWD | Age (ka) | Percent $^{39}Ar$ [steps, °C] | MSWD | $^{40}Ar/^{39}Ar_i$ | $^{40}Ar/^{39}Ar$ total gas |
| LC86-951 | Basalt of Penitentiary Flat | 16Z0319 | **130.0± 5.1** | 100 [550–1250] | 1.12 | 139.5 ± 7.1 | 100 [550–1250] | 0.85 | 295.7 ± 3.7 | 126.3 ± 5.8 |
| LC15-2591 | Basalt of Ice Cave Ridge | 16Z0193 | **127.5 ± 3.2** | 100 [550–1250] | 0.61 | 125.1 ± 3.9 | 100 [550–1250] | 0.55 | 299.5 ± 2.2 | 130.0 ± 4.1 |
| LC15-2592 | Basalt of Brockman Flat | 16Z0194 | **123.6 ± 18.7** | 76 [550–800] | 0.53 | 117.1 ± 31.2 | 100 [550–1250] | 1.8 | 296.8 ± 5.3 | 96.5 ± 23.7 |

Samples irradiated at U.S. Geological Survey TRIGA reactor using 9.797 Ma Bodie Hills sanidine as a neutron flux monitor, calibrated to GA1550. Sample LC15-2591 is from basalt of Ice Cave Ridge from the south vents. See figure 2 and table 1 for sample locations.

## Discussion

The basalt of Penitentiary Flat and the basalt of Ice Cave Ridge are petrographically similar olivine basalts. However, the basalt of Penitentiary Flat contains more abundant olivine and less abundant plagioclase phenocrysts, and lacks the abundant glomeroporphyritic clots identified within the basalt of Ice Cave Ridge. In addition, they are not in contact and their stratigraphic relation is unclear. The basalt of Brockman Flat overlies the basalt of Ice Cave Ridge, and is a tholeiitic, olivine basalt (often referred to as a low-potassium olivine tholeiite) with a diktytaxitic groundmass texture.

The combination of paleomagnetic, $^{40}Ar/^{39}Ar$, compositional, and petrographic data allows significant constraints to be placed on the age of the youngest Eagle Lake basalts. The basalt of Ice Cave Ridge, although erupted from two different sets of vents and with a slightly variable composition, represents a single eruption or two closely spaced eruptions at 127.5±3.2 ka. The similar paleomagnetic direction and composition of the basalt of Penitentiary Flat suggests that it is essentially the same age as the basalt of Ice Cave Ridge. Its simpler petrography suggests that it might have predated the basalt of Ice Cave Ridge, but not by more than a few decades.

Despite their petrographic differences, the basalt of Penitentiary Flat and the basalt of Ice Cave Ridge are compositionally similar and could be related to a similar magma batch (table 1) by fractionation. However, the compositional and petrographic differences between the basalt of Ice Cave Ridge and the basalt of Brockman Flat require them to be different magma batches (table 1). Although they have $^{40}Ar/^{39}Ar$ ages that are within uncertainty, their very different paleomagnetic directions require that they be significantly different in age, by at least several centuries and perhaps as much as several millennia, which is consistent with the $^{40}Ar/^{39}Ar$ ages.

The three young volcanic events at Eagle Lake all probably occurred within a span of, at most, a few millennia. The faulting that created the Eagle Lake basin is young (Grose, 2000), and the vent locations for the young basalts are clearly related to the lake basin boundary faults. However, only very minor movement on the basin-bounding faults has occurred since eruption of the young basalts. Thus, the faulting is mostly older than about 130 ka, but clearly younger than the basaltic andesite of Black Mountain, which erupted at 170±70 ka (Grose and McKee, 1986).

## Conclusions

The three youngest volcanic events at Eagle Lake represent an episode of volcanism at about 130–125 ka that lasted long enough for the basalt of Ice Cave Ridge and the basalt of Brockman Flat to have significantly different paleomagnetic directions. Although we cannot at present precisely determine the temporal extent of this episode, it is clear that it is not Holocene in age and is unlikely to have spanned more than a few thousand years. There have been no subsequent volcanic eruptions at Eagle Lake and only minor faulting since these young basalts were extruded. Thus, the short term potential for subsequent volcanism at Eagle Lake is considered low.

## Acknowledgments

We gratefully acknowledge peer reviews by U.S. Geological Survey colleagues Julie Donnelly-Nolan and Juliet Ryan-Davis. Samples for $^{40}Ar/^{39}Ar$ analysis were prepared by Katie Sullivan, and were irradiated by Brycen Roy and staff at the U.S. Geological Survey-TRIGA reactor in Denver, Colo.

## References

Clynne, M.A., and Muffler, L.J.P., 2010, Geologic map of Lassen Volcanic National Park and vicinity, California: U.S. Geological Survey Scientific Investigations Map I-2899, scale 1:50,000.

Clynne, M.A., Muffler, L.J.P., Siems, D.F., Taggart, J.E., Jr., and Bruggman, Peggy, 2008, Major and EDXRF trace element chemical analyses of volcanic rocks from Lassen Volcanic National Park and vicinity: U.S. Geological Survey Open-File Report 2008–1091, 11 p. and .xls table [Also available at http://pubs.usgs.gov/of/2008/1091/.]

Dalrymple, G.B., 1989, The GLM continuous laser system for $^{40}Ar/^{39}Ar$ dating—Description and performance characteristics, *in* Shanks, W.C., III, and Criss, R.E., eds., New frontiers in stable isotopic research—Laser probes, ion probes, and small-sample analysis: U.S. Geological Survey Bulletin 1890, p. 89–96.

Dalrymple, G.B., Alexander, E.C., Jr., Lanphere, M.A., and Kraker, G.P., 1981, Irradiation of samples for $^{40}Ar/^{39}Ar$ dating using the Geological Survey TRIGA reactor: U.S. Geological Survey Professional Paper 1176, 55 p.

Faulds, J.E., and Henry, C.D., 2008, Tectonic influences on the spatial and temporal evolution of the Walker Lane—An incipient transform fault along the evolving Pacific–North American plate boundary: Arizona Geological Digest 22, p. 437–470.

Fleck, R.J., and Calvert, A.T., 2016, Intercalibration of $^{40}Ar/^{39}Ar$ mineral standards with Bodie Hills sanidine [abs.]: Geological Society of America Annual Meeting, Abstract no. 238–4.

Grose, T.L.T., 2000, Volcanoes in the Susanville region, Lassen, Modoc, and Plumas Counties, northeastern California: California Geology, v. 53, no. 5, p. 4–23.

Grose, T.L.T., and McKee, E.H., 1986, Potassium-Argon ages of late Miocene to late Quaternary volcanic rocks in the Susanville-Eagle Lake area, Lassen County, California: Isochron/West, no. 45, p. 5–11.

Grose, T.L.T., Saucedo, G.J., and Wagner, D.L., 2008, Geologic map of the Eagle Lake 30' x 60' quadrangle, California, California: California Geological Survey, scale 1:100,000.

Grose, T.L.T., Saucedo, G.J., and Wagner, D.L., 2014, Preliminary geologic map of the Eagle Lake 30' x 60' quadrangle, Lassen County, California: California Geological Survey, pamphlet, 35 p., scale 1:100,000.

Guffanti, M., Clynne, M.A., Smith, J.G., Muffler, L.J.P., and Bullen, T.D., 1990, Late Cenozoic volcanism, subduction and extension in the Lassen region of California, Southern Cascade Range: Journal of Geophysical Research, v. 95, p. 19,453–19,464.

Johnson, D.M., Hooper, P.R., and Conrey, R.M., 1999, XRF analysis of rocks and minerals for major and trace elements on a single low dilution Li-tetraborate fused bead: Advances in X-ray Analysis, v. 41, p. 843–867.

Lee, J.-Y., Marti, K., Severinghaus, J.P., Kawamura, K., Yoo, H.-S., Lee, J.B., and Kim, J.S., 2006, A redetermination of the isotopic abundances of atmospheric Ar: Geochimica et Cosmochimica Acta, v. 70, p. 4507–4512.

McDougall, I., and Wellman, P., 2011, Calibration of GA1550 biotite standard for K/Ar and $^{40}Ar/^{39}Ar$ dating: Chemical Geology, v. 280, p. 19–25.
McElhinny, M.W., 1973, Paleomagnetism and plate tectonics: Cambridge University Press, 368 p.
Miller, C.D., 1989, Potential hazards from future volcanic eruptions in California: U.S. Geological Survey Bulletin 1847, 17 p.
Muffler, L.J.P., and Clynne, M.A., 2015, Geologic field-trip guide to Lassen Volcanic National Park and vicinity, California: U.S. Geological Survey Scientific Investigations Report 2015–5067, 67 p., http://dx.doi.org/10.3133/sir21055067.
Stovall, W.K., Marcaida, M., and Mangan, M.T., 2014, The California Volcano Observatory–Monitoring the State's restless volcanoes: U.S. Geological Survey Fact Sheet 2014–3120, 4 p.
Turrin, B.D., Muffler, L.J.P., Clynne, M.A., and Champion, D.E., 2007, Robust 24 ± 6 ka $^{40}Ar/^{39}Ar$ age of a low-potassium tholeiitic basalt in the Lassen region of NE California: Quaternary Research, v. 68, p. 96–110.

# Appendix 1. $^{40}Ar/^{39}Ar$ Analytical Techniques

The $^{40}Ar/^{39}Ar$ geochronology was performed using crystalline groundmass that was segregated by crushing, sieving, heavy liquid, and magnetic techniques. Samples were carefully handpicked under a binocular microscope. For irradiation, ~200 milligrams (mg) of separates were packaged in copper foil and placed in a cylindrical quartz vial, together with fluence monitors of known age and potassium-glass and fluorite to measure interfering isotopes from potassium and calcium. The quartz vials were wrapped in 0.5 millimeter (mm)-thick cadmium foil to shield samples from thermal neutrons during irradiation. The samples were irradiated for one hour in the central thimble of the U.S. Geological Survey TRIGA reactor in Denver, Colo. (Dalrymple and others, 1981). The reactor vessel was rotated continuously during irradiation to avoid lateral neutron flux gradients and oscillated vertically to minimize vertical gradients. Reactor constants determined for these irradiations were indistinguishable from recent irradiations, and a weighted mean of constants obtained over the past five years yields $^{40}Ar/^{39}Ar_K = 0.0010\pm0.0004$, $^{39}Ar/^{37}Ar_{Ca} = 0.00071\pm0.00005$, and $^{36}Ar/^{37}Ar_{Ca} = 0.000281\pm0.000006$. Bodie Hills sanidine (Fleck and Calvert, 2016) was used as a fluence monitor with an age of 9.797 Ma. Bodie Hills sanidine is a secondary standard calibrated against the primary intralaboratory standard, GA1550 biotite, that has an age of 98.79±0.96 Ma (McDougall and Wellman, 2011). Fluence monitors and unknowns were analyzed using a continuous $CO_2$ laser system and mass spectrometer described by Dalrymple (1989). Gas was purified continuously during extraction using two SAES ST-175 getters operated at 4 amperes and 0 amperes.

Mass spectrometer discrimination and system blanks are important factors in the precision and accuracy of $^{40}Ar/^{39}Ar$ age determinations of Pleistocene samples because of low radiogenic yields. Discrimination is monitored by analyzing splits of atmospheric argon from a reservoir attached to the extraction line and for these samples $D_{1amu} = 1.010795 \pm 0.000169$. Typical system blanks including mass spectrometer backgrounds were $1.5x10^{-18}$ mol of m/z 36, $9x10^{-17}$ mol of m/z 37, $3x10^{-18}$ mol of m/z 39 and $1.5x10^{-16}$ mol of m/z 40, where m/z is mass/charge ratio.

# Appendix 2. Tabulated $^{40}Ar/^{39}Ar$ data for basaltic flows of Eagle Lake

[Temp, temperature; °C, degrees Celsius; ka, thousand years; %, percent]

| LC86-951 basalt of Penitentiary Flat (unit bpf) | | | | | | | | | | | |
|---|---|---|---|---|---|---|---|---|---|---|---|
| Temp (°C) | Age (ka) | $\%^{40}Ar^*$ | K/Ca | K/Cl | moles $^{40}Ar^*$ | $\Sigma^{39}Ar$ | $^{40}Ar$ | $^{39}Ar$ | $^{38}Ar$ | $^{37}Ar$ | $^{36}Ar$ |
| 550 | 139.4±123.2 | 6.12 | 0.11 | -1512 | 3.05E-16 | 0.01 | 0.070045± 0.000398 | 0.012315± 0.000046 | 0.000170± 0.000026 | 0.058517± 0.001198 | 0.000237± 0.000013 |
| 650 | 145.4±14.5 | 11.27 | 0.11 | -16619 | 3.96E-15 | 0.14 | 0.494033± 0.000347 | 0.153271± 0.000167 | 0.002266± 0.000050 | 0.716228± 0.000692 | 0.001669± 0.000018 |
| 725 | 128.3±9.6 | 14.23 | 0.12 | -77245 | 5.18E-15 | 0.34 | 0.511737± 0.000281 | 0.227055± 0.000196 | 0.003270± 0.000063 | 1.021561± 0.003137 | 0.001757± 0.000017 |
| 775 | 129.9±10.5 | 15.47 | 0.16 | -9214 | 4.62E-15 | 0.52 | 0.420021± 0.000299 | 0.199976± 0.000206 | 0.002772± 0.000087 | 0.652030± 0.001907 | 0.001372± 0.000017 |
| 825 | 128.3±9.5 | 13.67 | 0.21 | -7937 | 5.01E-15 | 0.71 | 0.515391± 0.000255 | 0.219415± 0.000171 | 0.003056± 0.000135 | 0.556121± 0.003997 | 0.001646± 0.000017 |
| 875 | 148.2±14.8 | 11.87 | 0.18 | -9653 | 3.94E-15 | 0.84 | 0.466215± 0.000264 | 0.149213± 0.000157 | 0.002162± 0.000043 | 0.445285± 0.001931 | 0.001501± 0.000018 |
| 950 | 96.5±27.0 | 3.65 | 0.10 | 5820 | 1.51E-15 | 0.91 | 0.581431± 0.000292 | 0.088146± 0.000115 | 0.001585± 0.000064 | 0.469972± 0.001280 | 0.002008± 0.000020 |
| 1050 | 51.4±37.6 | 1.05 | 0.09 | 1792 | 4.93E-16 | 0.96 | 0.663247± 0.000299 | 0.054040± 0.000084 | 0.001258± 0.000037 | 0.324969± 0.001348 | 0.002289± 0.000017 |
| 1150 | 58.5±65.2 | 0.69 | 0.04 | 458 | 3.77E-16 | 0.99 | 0.766854± 0.000402 | 0.036396± 0.000073 | 0.001304± 0.000055 | 0.432617± 0.001755 | 0.002672± 0.000020 |
| 1250 | 287.1±333.7 | 0.96 | 0.00 | 394 | 3.80E-16 | 1.0 | 0.557592± 0.000331 | 0.008115± 0.000043 | 0.000556± 0.000045 | 0.967353± 0.003299 | 0.002121± 0.000020 |

Packet IRR357-TE, Experiment #16Z0319, 0.1892 g basalt, all errors ±1 sigma

J = 0.000221150345±0.000000290016

$^{40}Ar^*$ is radiogenic argon, isotopes in volts (7.12E-14 moles/volt), corrected for blank, background, discrimination and decay

Calculated bulk K/Ca = 0.106±3.776E-2, Calculated $K_2O$ = 0.75 weight percent, Calculated CaO = 8.62 weight percent, Calculated Cl = -4.3E-2 parts per million

Total gas age = 126.3±5.8 ka

**Weighted mean plateau age = 130.0±5.1 ka (±1 sigma, including ±J), 100.0 percent $^{39}Ar$ released**

Weighted mean plateau age = 130.0±4.8 ka (a priori, ±1 sigma, including ±J), 100.0 percent $^{39}Ar$ released

Weighted mean plateau age = 130.0±11.8 ka (95 percent confidence, including ±J)

Mean square of the weighted deviates (MSWD) = 1.12 (Good fit, MSWD <2.11)
Steps 10 of 10 (550, 650, 725, 775, 825, 950, 1050, 1150, 1250 °C)
Isochron age = 139.5±7.1 ka (±1 sigma, including ±J)
Isochron age = 139.5±7.1 ka (a priori, including ±J)
Isochron age = 139.5±16.9 ka (95 percent confidence, including ±J)
MSWD = 0.85 (Good fit, MSWD <2.19)
$^{40}Ar/^{36}Ar$ intercept = 295.7±1.6 (±1 sigma)
$^{40}Ar/^{36}Ar$ intercept = 295.7±1.6 (a priori)
$^{40}Ar/^{36}Ar$ intercept = 295.7±3.7 (95 percent confidence)
Steps 10 of 10 (550, 650, 725, 775, 825, 950, 1050, 1150, 1250 °C)

| LC15-2591 basalt of Ice Cave Ridge from the south vents (unit bics) | | | | | | | | | | | |
|---|---|---|---|---|---|---|---|---|---|---|---|
| Temp (°C) | Age (ka) | %$^{40}$Ar* | K/Ca | K/Cl | moles $^{40}$Ar* | Σ$^{39}$Ar | $^{40}$Ar | $^{39}$Ar | $^{38}$Ar | $^{37}$Ar | $^{36}$Ar |
| 550 | 137.8±27.3 | 11.24 | 0.18 | -6005 | 1.40E-15 | 0.03 | 0.084095±0.000087 | 0.028486±0.000052 | 0.000403±0.000011 | 0.083907±0.000194 | 0.000274±0.000006 |
| 625 | 120.2±10.3 | 15.28 | 0.18 | -4594 | 4.08E-15 | 0.13 | 0.180264±0.000264 | 0.095151±0.000095 | 0.001264±0.000022 | 0.277349±0.000619 | 0.000589±0.000008 |
| 700 | 122.8±6.7 | 19.37 | 0.18 | -7668 | 7.87E-15 | 0.32 | 0.274623±0.000224 | 0.179849±0.000130 | 0.002413±0.000024 | 0.513899±0.000714 | 0.000886±0.000009 |
| 750 | 125.5±5.8 | 20.46 | 0.27 | -10592 | 9.29E-15 | 0.54 | 0.307227±0.000249 | 0.207733±0.000118 | 0.002808±0.000030 | 0.400811±0.000295 | 0.000931±0.000009 |
| 800 | 128.4±7.3 | 18.06 | 0.38 | -19016 | 6.86E-15 | 0.70 | 0.256910±0.000140 | 0.149944±0.000115 | 0.002073±0.000021 | 0.205752±0.000322 | 0.000762±0.000009 |
| 850 | 134.2±11.6 | 14.28 | 0.39 | -10638 | 4.61E-15 | 0.80 | 0.218101±0.000140 | 0.096261±0.000094 | 0.001346±0.000036 | 0.129773±0.000280 | 0.000662±0.000009 |
| 925 | 152.3±13.5 | 9.39 | 0.33 | 23545 | 4.03E-15 | 0.88 | 0.289811±0.000181 | 0.074137±0.000079 | 0.001155±0.000027 | 0.117165±0.000365 | 0.000912±0.000008 |
| 1000 | 142.2±34.4 | 4.37 | 0.23 | -11904 | 1.79E-15 | 0.92 | 0.276249±0.000176 | 0.035245±0.000070 | 0.000618±0.000023 | 0.081936±0.000483 | 0.000908±0.000010 |
| 1100 | 122.6±33.4 | 2.25 | 0.16 | 4130 | 2.26E-15 | 0.97 | 0.679637±0.000260 | 0.051757±0.000067 | 0.001154±0.000021 | 0.171812±0.000770 | 0.002273±0.000014 |
| 1250 | 173.6±77.6 | 0.8 | 0.02 | 422 | 1.49E-15 | 1.0 | 1.263977±0.000418 | 0.024529±0.000064 | 0.001357±0.000032 | 0.670855±0.001971 | 0.004388±0.000014 |

Packet IRR351-OD, Experiment #16Z0193, 0.2024 g basalt, all errors ±1 sigma

J = 0.000229844384710±3.4332E-07

$^{40}$Ar* is radiogenic argon, isotopes in volts (1.48E-13 moles/volt), corrected for blank, background, discrimination and decay

Calculated bulk K/Ca = 0.186±7.284E-2, Calculated $K_2O$ = 1.44 weight percent, Calculated CaO = 9.46 weight percent, Calculated Cl = -3.1E-2 parts per million

Total gas age = 130.0±4.1 ka

**Weighted mean plateau age = 127.5±3.2 ka (±1 sigma, including ±J), 100.0 percent $^{39}$Ar released**

Weighted mean plateau age = 127.5±3.2 ka (a priori, ±1 sigma, including ±J), 100.0 percent $^{39}$Ar released

Weighted mean plateau age = 127.5±5.8 ka (95 percent confidence, including ±J)

Mean square of the weighted deviates (MSWD) = 0.61 (Good fit, MSWD <2.11)

Steps 10 of 10 (550, 625, 700, 750, 800, 925, 1000, 1100, 1250 °C)

Isochron age = 125.1±3.9 ka (±1 sigma, including ±J)

Isochron age = 125.1±3.9 ka (a priori, including ±J)

Isochron age = 125.1±3.9 ka (95 percent confidence, including ±J)

MSWD = 0.55 (Good fit, MSWD <2.19)

$^{40}Ar/^{36}Ar$ intercept = 299.5±0.9 (±1 sigma)

$^{40}Ar/^{36}Ar$ intercept = 299.5±0.9 (a priori)

$^{40}Ar/^{36}Ar$ intercept = 299.5±2.2 (95 percent confidence)

Steps 10 of 10 (550, 625, 700, 750, 800, 925, 1000, 1100, 1250 °C)

| LC15-2592 basalt of Brockman Flat (unit bbf) | | | | | | | | | | | |
|---|---|---|---|---|---|---|---|---|---|---|---|
| Temp (°C) | Age (ka) | %$^{40}$Ar* | K/Ca | K/Cl | moles $^{40}$Ar* | Σ$^{39}$Ar | $^{40}$Ar | $^{39}$Ar | $^{38}$Ar | $^{37}$Ar | $^{36}$Ar |
| 550 | 152.3±112.4 | 5.04 | 0.03 | 3964 | 3.60E-16 | 0.04 | 0.048272±0.000069 | 0.006705±0.000024 | 0.000126±0.000012 | 0.102119±0.000589 | 0.000182±0.000006 |
| 625 | 183.6±49.3 | 8.25 | 0.03 | 3323 | 1.29E-15 | 0.17 | 0.105602±0.000115 | 0.019935±0.000043 | 0.000356±0.000013 | 0.327731±0.000687 | 0.000417±0.000008 |
| 700 | 119.1±32.0 | 6.64 | 0.03 | 55377 | 1.54E-15 | 0.40 | 0.156245±0.000128 | 0.036581±0.000071 | 0.000589±0.000014 | 0.585579±0.000977 | 0.000653±0.000009 |
| 750 | 117.5±35.2 | 6.09 | 0.04 | -6432 | 1.30E-15 | 0.60 | 0.144210±0.000138 | 0.031306±0.000070 | 0.000485±0.000018 | 0.410012±0.000977 | 0.000569±0.000008 |
| 800 | 93.6±41.3 | 3.3 | 0.06 | -8089 | 8.04E-16 | 0.76 | 0.164729±0.000124 | 0.024246±0.000037 | 0.000411±0.000020 | 0.229463±0.000423 | 0.000598±0.000008 |
| 850 | -110.5±74.9 | -2.3 | 0.06 | -14894 | -4.95E-16 | 0.84 | 0.144546±0.000120 | 0.012544±0.000032 | 0.000256±0.000016 | 0.110070±0.000796 | 0.000526±0.000007 |
| 925 | -20.4±117.9 | -0.23 | 0.04 | 2209 | -7.00E-17 | 0.90 | 0.205790±0.000151 | 0.009697±0.000025 | 0.000278±0.000016 | 0.112969±0.000564 | 0.000723±0.000009 |
| 1025 | -75.1±167.7 | -0.56 | 0.03 | 1354 | -1.79E-16 | 0.94 | 0.214642±0.000163 | 0.006784±0.000026 | 0.000248±0.000012 | 0.118438±0.000287 | 0.000756±0.000009 |
| 1100 | -36.8±227.5 | -0.18 | 0.02 | 503 | -6.30E-17 | 0.97 | 0.235130±0.000155 | 0.004885±0.000025 | 0.000256±0.000015 | 0.126074±0.000507 | 0.000824±0.000009 |
| 1250 | 544.3±476.6 | 0.84 | 0 | 103 | 8.67E-16 | 1.0 | 0.698568±0.000254 | 0.005473±0.000023 | 0.000725±0.000022 | 1.415970±0.001359 | 0.002718±0.000015 |

Packet IRR351-OG, Experiment #16Z0194, 0.1958 g basalt, all errors ±1 sigma

J = 0.000230143919695±4.2199E-07

$^{40}$Ar* is radiogenic argon, isotopes in volts (1.48E-13 moles/volt), corrected for blank, background, discrimination and decay

Calculated bulk K/Ca = 2.308±1.084E-2, Calculated $K_2O$ = 0.24 weight percent, Calculated CaO = 12.60 weight percent, Calculated Cl = 0.1 parts per million

Total gas age = 96.5±23.7 ka

**Weighted mean plateau age = 123.6±18.7 ka (±1 sigma, including ±J), 75.5 percent $^{39}$Ar released**

Weighted mean plateau age = 123.6±18.7 ka (a priori, including ±J), 75.5 percent $^{39}$Ar released

Weighted mean plateau age = 127.5±5.8 ka (95 percent confidence, including ±J)

Mean square of the weighted deviates (MSWD) = 0.53 (Good fit, MSWD <2.77)

Steps 5 of 10 (550, 625, 700, 750, 800 °C)

Isochron age = 146.8±89.2 ka (±1 sigma, including ±J)

Isochron age = 146.8±89.2 ka (a priori, including ±J)

Isochron age = 146.8±210.9 ka (95 percent confidence, including ±J)

MSWD = 0.66 (Good fit, MSWD <3.12)

$^{40}Ar/^{36}Ar$ intercept = 295.0±12.9 (±1 sigma)

$^{40}Ar/^{36}Ar$ intercept = 295.0±12.9 (a priori)

$^{40}Ar/^{36}Ar$ intercept = 295.0±30.5 (95 percent confidence)

Steps 5 of 10 (550, 625, 700, 750, 800 °C)